A Survey Report on Negative-Refractive-Index Transmission-Line Metamaterials and Applications

Microwave and Millimeter Techniques (ECE 1236)

Instructor: Professor George Eleftheriades

Xiuquan Zhang (996922399)

Alireza Zandieh (1002506558)

Abstract

Metamaterials (meta means “beyond” or “after” in Greek) are a new class of synthetic materials that have peculiar electromagnetic properties not typically found in nature. They have captured much attention within the science and engineering communities for their potential to create new devices that exhibit superior qualities compared to the traditional materials.

The development of metamaterials has been regarded as one of the top ten scientific breakthroughs by Science magazine in 2003 [1]. Being different from traditional materials, metamaterials are characterized by a negative effective permittivity and simultaneously a negative effective permeability over a certain frequency band. The electric field $\vec{E}$, magnetic field $\vec{H}$ and wave vector $\vec{k}$ in these materials form a left-handed triplet, such that the direction of phase velocity $\vec{v}_p$ is opposite to the direction of group velocity $\vec{v}_g$. Thus, they exhibit many unusual properties such as negative refraction of electromagnetic wave, reversed Doppler effect, reversed Cherenkov radiation, perfect lens effect and etc. These metamaterials are often referred to as **NRI** (negative refractive index), **DNG** (double negative) material, **BW** (backward) media, and **LH** (left-handed) media, to name a few. The NRI metamaterials have created intense research activities over the past two decades as many have attempted to incorporate material with such characteristics to design or enhance the performance of lenses, microwave devices, phase shifters, broadband power dividers, backward and forward leaky-wave antennas, electrically small ring antennas, cloaking, and miniaturization [2–7].

This survey report mainly focuses on the negative-refractive-index transmission-line (NRI-TL) metamaterial, which is a subtype of metamaterials, and provides an introductory overview of the topic including its historical background and development, the underlying theories, the applications in antenna and microwave devices, and future directions.

Contents

1. Introduction

1.1 Motivation of Using Metamaterials

The ongoing development of the next-generation wireless communication systems is bringing about many challenges. On one hand, designers and customers have always been looking for smaller and multifunctional wireless devices, and even want them to become wearable. An example is about how to integrate multiple antennas and RF components in a mobile handset, yet still maintains its aesthetical appeal, efficiency and broadband/multi-band functionalities. Reducing antenna profile via traditional miniaturization techniques such as shorting pins [8], meandering [9], and dielectric loading [10] often result in low radiation efficiencies, narrow bandwidth, and undesired radiation patterns.

On the other hand, for imaging applications, the resolution of lenses built of conventional materials is always diffraction limited even if they are well designed. This is due to the fact that conventional lenses only rely on the collection and interference of propagating waves, but the evanescent waves containing the finest spatial details of the source decay rapidly and lost.

It is not therefore surprising that strong interest exists in engineered materials such as metamaterials as a method to optimize or enhance the performance of antennas, microwave devices and lenses.

1.2 Historical Perspective of Metamaterials

The pursuit of artificial materials for electromagnetic applications can be traced back to Jadagis Chunder Bose in 1898 when he worked and experimented on the constructed twisted elements that exhibit properties nowadays known as chiral characteristics [11]. In 1914, Lindman studied wave interaction with collections of metallic helices as artificial chiral media [12]. In 1948, Kock of Bell Laboratories made lightweight microwave lenses by arranging conducting spheres, disks, and strips periodically and effectively tailoring the effective refractive index of the artificial media [13]. Since then, artificial complex materials have been the subject of research for many investigators worldwide.

In 1967, Victor Veselago, a Russian physicist of Lebedev Physical Institute theoretically investigated plane-wave propagation in a material whose permittivity and permeability were assumed to be simultaneously negative [14]. His study showed that for a monochromatic uniform plane wave in such medium the direction of the Poynting vector is antiparallel to the direction of the phase velocity, contrary to the case of plane wave propagation in conventional simple media as illustrated in Fig. 1. He referred to such materials as left-handed. However, he did not speculate, at least in [14], how and what kind of materials may exhibit left-handed properties.

The work of Veselago remained dormant for about 30 years, and it was not until the late 1990s when John Pendry and his colleagues pointed out that DNG materials could be created artificially by using periodic structures [15–18]. Not long after Pendry, David Smith and his colleagues [19–23] of University of California, San Diego built the first left-handed material that exhibited DNG

characteristics at microwave frequencies. This was accomplished by using a structure consisting of split-ring resonators (SRRs) and wires, a unit cell of which is shown in Fig. 1. It was suggested that the SRR oriented normal to the plane of the rings will contribute a negative permeability while the infinite length wire will contribute a negative permittivity; the combination of the two will, in a periodic structure, contribute a negative index-of-refraction.

Year 2003 was the golden year for metamaterial research in which many discoveries and breakthroughs were achieved. A group led by G.V. Eleftheriades at the University of Toronto, and other groups led by Arthur A. Oliner of Polytechnic Institute of New York University and T. Itoh of University of California, Los Angeles separately developed a transmission line approach to form a negative-index-refractive metamaterial. It was based on the concept of periodically loading a conventional microwave transmission line (TL) with series capacitors and shunt inductors, as shown in Fig. 2b. This transmission-line approach has demonstrated that a large bandwidth can be obtained over which the refractive index remains negative. In addition, it has also lower transmission losses through the media than in the original wire/SRR media []. This is because the transmission-line approach does not rely on loosely coupled resonators to synthesize the negative permeability, but rather it depends on the tight coupling between adjacent resonant loops that are formed by loading the host transmission line with series capacitors and shunt inductors [24].

Due to the smaller transmission loss and larger left-handed frequency bandwidth, NRI-TL metamaterials are much more applicable implementing antenna microwave devices.

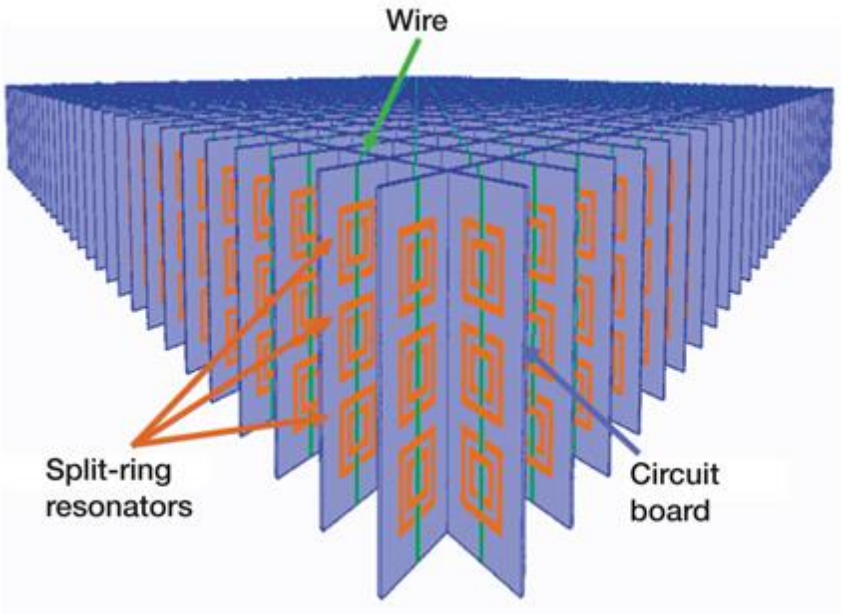

Fig. 1 A split-ring resonator and wire based NRI metamaterial.

2. Negative-Refractive-Index Transmission-Line Theory

2.1 One-dimensional Transmission-line Model

Because metamaterials are effectively homogeneous structures, they can be modeled by one-dimensional (1D) transmission lines (TLs), whose propagation direction represents any direction in the material. A transmission-line based LHM is the dual of the conventional right-handed (RH) LC network, and has series capacitance and shunt inductance as shown in Fig. 2(a) and (b). Due to the parasitic effects of the host medium, NRI metamaterials also support ordinary RH wave propagation at higher frequencies, a purely LH (PLH) does not exist. Therefore, a more realistic model, the so-called composite right/left-handed (CRLH) structure [25], was introduced and as sown in Fig. 2(c).

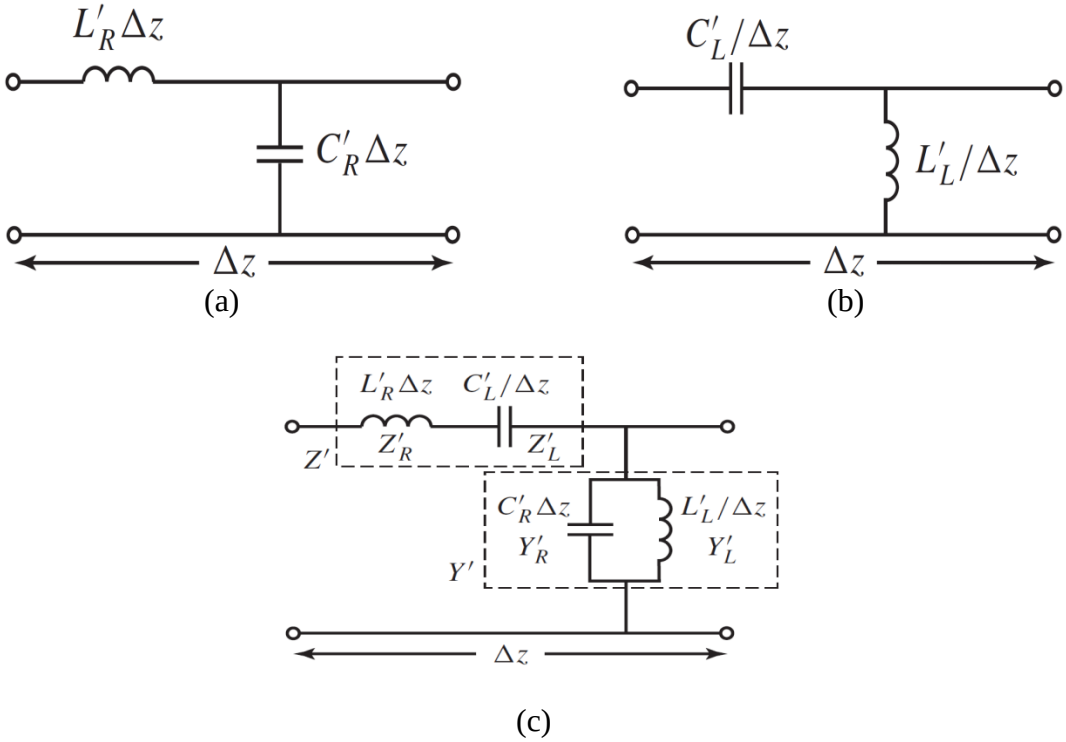

Fig. 2 *Equivalent circuit model. (a) Homogeneous RH TL. (b) Homogeneous LH TL. (c) Homogeneous CRLH TL.*

The L'_R, C'_R in Fig. 2 are per-unit length series inductance and shunt capacitance, which are responsible for RH propagation at higher frequencies, whereas L'_L, C'_L are times-unit length shunt inductance, which are responsible for LH propagation at lower frequencies. The propagation constant of a TL is given by:

$$\gamma = \alpha + j\beta = \sqrt{Z'Y'} \tag{1}$$

where Z' and Y' are, respectively, the per-unit length impedance and per-unit length admittance. In the particular case of the CRLH TL, Z' and Y' are defined as:

$$Z'(\omega) = j\left(\omega L'_R - \frac{1}{\omega C'_R}\right)$$
$$Y'(\omega) = j\left(\omega C'_R - \frac{1}{\omega L'_R}\right) \quad (2)$$

Suppose the TL is lossless, then $\alpha = 0$, and substitute (2) into (1), the dispersion relation for a homogenous CRLH TL is:

$$\beta(\omega) = s(\omega)\sqrt{\omega^2 L'_R C'_R + \frac{1}{\omega^2 L'_L C'_L} - \left(\frac{L'_R}{L'_L} + \frac{C'_R}{C'_L}\right)} \quad (3)$$

where

$$s(\omega) = \begin{cases} -1, \text{if } \omega < \omega_{\Gamma 1} = \min\left(\frac{1}{\sqrt{L'_R C'_L}}, \frac{1}{\sqrt{L'_L C'_R}}\right) \\ 1, \text{ if } \omega < \omega_{\Gamma 2} = \max\left(\frac{1}{\sqrt{L'_R C'_L}}, \frac{1}{\sqrt{L'_L C'_R}}\right) \end{cases} \quad (4)$$

from the equation above, we can conclude that:

a. When $\omega^2 L'_R C'_R + \frac{1}{\omega^2 L'_L C'_L} - \left(\frac{L'_R}{L'_L} + \frac{C'_R}{C'_L}\right) > 0$, $\beta(\omega)$ is real and $\gamma = j\,\beta(\omega)$ is imaginary, then there exists a pass-band.
b. When $\omega^2 L'_R C'_R + \frac{1}{\omega^2 L'_L C'_L} - \left(\frac{L'_R}{L'_L} + \frac{C'_R}{C'_L}\right) < 0$, $\beta(\omega)$ is imaginary and $\gamma = j\,\beta(\omega)$ is real, then there exists a stop-band.

For a RH TL, its phase constant is:

$$\beta_R(\omega) = \omega\sqrt{L'_R C'_R} \quad (5)$$

and for a LH TL, its phase constant is:

$$\beta_L(\omega) = -\frac{1}{\omega\sqrt{L'_L C'_L}} \quad (6)$$

according to the definitions of group and phase velocities:

$$v_g = \frac{\partial\omega}{\partial\beta} \text{ and } v_p = \frac{\omega}{\beta} \quad (7)$$

substitute (6) into (7), we can obtain that for a RH TL $v_g = v_p = \frac{1}{\sqrt{L'_R C'_R}}$, such that the group and phase velocities have the same direction. And for for a LH TL $v_g = -v_p = \omega^2\sqrt{L'_R C'_R}$, such that the group and phase velocities have opposite directions.

Based on equations (5), (6) and (3), dispersion relations between $\beta(\omega)$ and ω for RH TL, LH TL and CRLH TL are illustrated as follows:

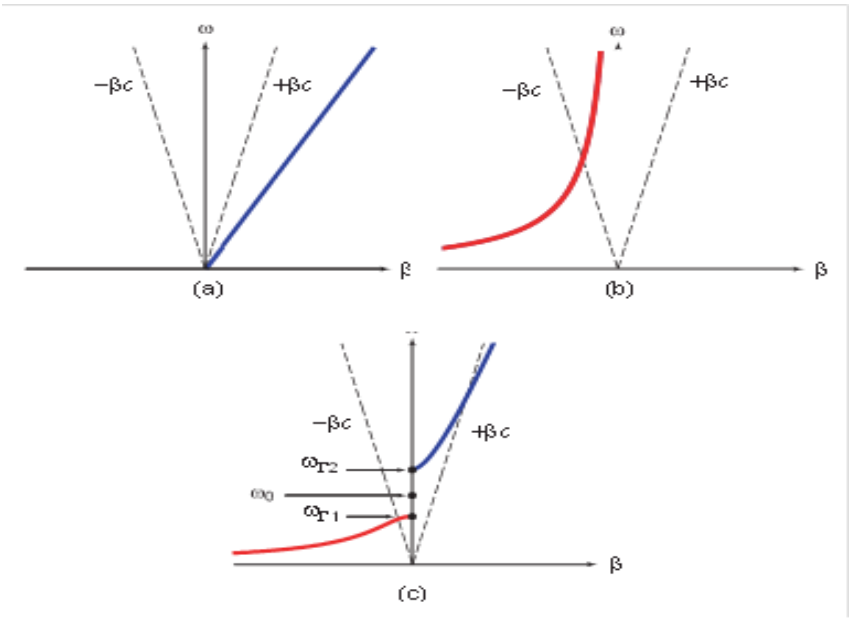

Fig. 3 *Dispersion diagrams for (a) Homogeneous RH TL. (b) Homogeneous LH TL. (c) Homogeneous CRLH TL (unbalanced).*

In general, the series and shunt resonances of the CRLH TL are different. This is called the unbalanced case. When the series and shunt resonances are equal, such that $L'_R C'_L = L'_L C'_R = L'C'$, we have balanced condition, and the phase constant $\beta(\omega)$ can be simplified as:

$$\beta(\omega) = \beta_R(\omega) + \beta_R(\omega) = \omega\sqrt{L'_R C'_R} - \frac{1}{\omega\sqrt{L'_L C'_L}} \tag{8}$$

From equation (8) above, when $\omega \to 0$, or at low frequencies, the CRLH TL exhibits LH behaviour, and when $\omega \to +\infty$, or at high frequencies, the CRLH TL exhibits RH behaviour. Of course, the LH and RH propagation properties can be tuned to some desired frequency range by simply controlling the unit cell parameters such as the amount of the reactive loads. The transition from LH to RH occurs when:

$$\omega_0 \overset{\text{unbalanced}}{=} \frac{1}{4\sqrt{L'_R C'_R L'_L C'_L}} \overset{\text{balanced}}{=} \frac{1}{\sqrt{L'C'}} \tag{9}$$

where ω_0 is the transition frequency and $\beta(\omega_0) = 0$.

The equivalent circuit and dispersion relation for CRLH TL under balanced condition are given in Fig. 4 as follows:

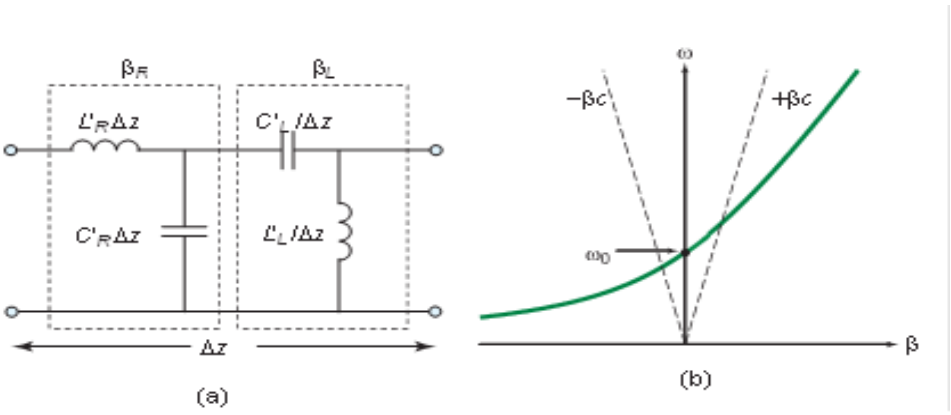

Fig. 4 *Balanced form of CRLH TL. (a) Simplified equivalent circuit model. (b) Dispersion diagram showing seamless LH to RH transition.*

From the characteristic impedance of the TL, $Z_0 = \sqrt{Z'/Y'}$, the characteristic impedance of the CRLH TL is given as:

$$Z_0 = \sqrt{\frac{Z'}{Y'}} = Z_L\sqrt{\frac{L'_R C'_L \omega^2 - 1}{L'_L C'_R \omega^2 - 1}} \tag{10}$$

the characteristic impedance of the RH TL is:

$$Z_0 = \sqrt{\frac{Z'}{Y'}} = \sqrt{\frac{L'_R}{C'_R}} \tag{11}$$

the characteristic impedance of the RH TL is:

$$Z_0 = \sqrt{\frac{Z'}{Y'}} = \sqrt{\frac{L'_L}{C'_L}} \tag{12}$$

and under the balanced condition, the characteristic impedance of the CRLH TL is:

$$Z_0 = Z_R = Z_L \tag{13}$$

Also from $\beta = \omega\sqrt{\mu\varepsilon}$ and $\gamma = \sqrt{Z'Y'} = j\,\beta$, the following relation can be established:

$$Z'Y' = -\,\omega^2\mu\varepsilon \tag{14}$$

Since the intrinsic impedance of the metamaterial is $\eta = \sqrt{\mu/\varepsilon}$, if we equate it with the characteristic impedance of the TL, $Z_0 = \sqrt{Z'/Y'}$, such that $Z_0 = \eta$, then we have:

$$\frac{Z'}{Y'} = \frac{\mu}{\varepsilon} \tag{15}$$

From the above analysis, the permeability and permittivity of the CRLH TL are:

$$\mu = \frac{Z'}{j\omega} = L'_R - \frac{1}{\omega^2 C'_L} \tag{16a}$$

$$\varepsilon = \frac{Y'}{j\omega} = C'_R - \frac{1}{\omega^2 L'_L} \tag{16b}$$

From the definition of index of refraction $n = c\beta/\omega$ and equation (8), we have:

$$n_{CRLH} = \frac{1}{\sqrt{\mu_0 \varepsilon_0}} \left(\sqrt{L'_R C'_R} - \frac{1}{\omega^2 \sqrt{L'_L C'_L}} \right) \tag{17}$$

And when $\omega \to 0$, or at low frequencies:

$$n_{CRLH} \approx n_{LH} = -\frac{1}{\omega^2 \sqrt{L'_L C'_L \mu_0 \varepsilon_0}} \tag{18}$$

which gives the negative index of refraction.

2.2. Two-dimensional Transmission-line Model

The 2-D CRLH TL is just an extension of the 1-D case. Similar to the design of a 1-D CRLH TL, a 2-D CRLH TL can be constructed by repeating the 2-D unit cell of Fig. 5(a) along two directions as shown in Fig. 5(b). The 2-D CRLH TL supports wave propagation in any direction within the structure. As a result, the phase constant β is a vector quantity, such that $\vec{\beta} = k_x\hat{x} + k_y\hat{y}$, where k_x and k_y are the propagation constants for the x and y directions. Using Bloch-Floquet periodic boundary conditions and ABCD matrices of the 2-D unit cell along the x and y directions, the 2-D dispersion relation is:

$$\frac{\left(e^{-jk_x p_x} - 1\right)^2}{e^{-jk_x p_x}} + \frac{\left(e^{-jk_y p_y} - 1\right)^2}{e^{-jk_y p_y}} + \chi = 0 \tag{19}$$

where p_x and p_y are the unit cell periods along x and y directions as shown in Fig. , and

$$\chi = \left(\frac{\omega}{\omega_R}\right)^2 + \left(\frac{\omega_L}{\omega}\right)^2 - \kappa\omega_L^2, \text{ with} \tag{20a}$$

$$\omega_R = \frac{1}{\sqrt{L_R C_R}}, \tag{20b}$$

$$\omega_L = \frac{1}{\sqrt{L_L C_L}}, \tag{20c}$$

$$\kappa = L_R C_L + L_L C_R. \tag{20d}$$

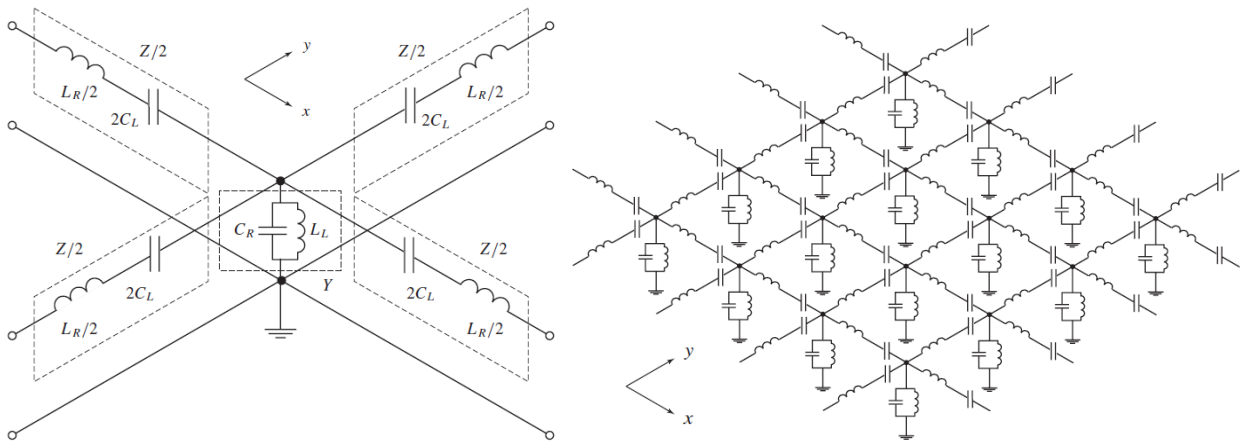

Fig. 5 *(a) Unit cell of a CRLH 2D periodic network TL. (b) 2D CRLH periodic network consisting by the repetition of the unit cell of along both the x and y directions.*

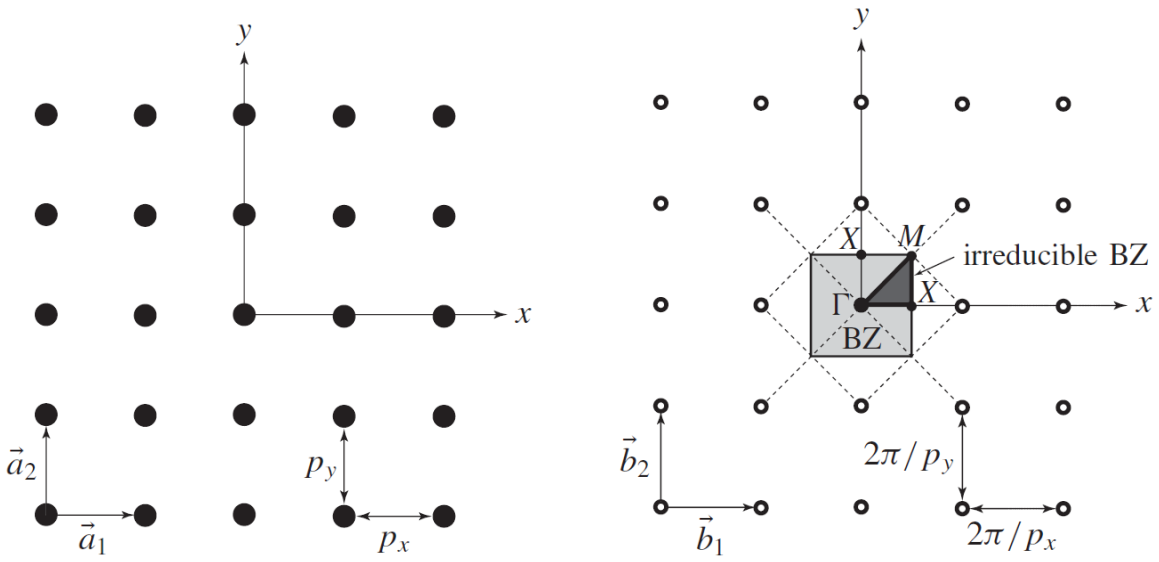

Fig. 6 Square lattices for a 2D structure. (a) Direct (spatial) lattice. (b) Reciprocal (spectral) lattice.

For simplicity, choose the square lattice network to represent 2-D CRLH TL network, the direct (or spatial) lattice is shown in Fig. 6(a), and the reciprocal (spectral) lattice is shown in Fig. 6(b). Fig. 6(b) also shows the Brillouin zone (BZ) of the periodic lattice, which is the square surface $[-\pi/p_x < k_x < +\pi/p_x, -\pi/p_y < k_y < +\pi/p_y]$. Due to symmetry, this BZ can be reduced to the triangular surface shown in the figure, which is called the irreducible Brillouin zone. This irreducible zone is further reduced to the segment Γ-X-M-Γ, where Γ ($k_xp_x = k_yp_y = 0$), X ($k_xp_x = \pi$, $k_yp_y = 0$), and M ($k_xp_x = k_yp_y = \pi$) represent the high-symmetry points of the BZ. The structure is LH from $\omega_{\Gamma 1}$ to ω_{M1} and RH from $\omega_{\Gamma 2}$ to ω_{M2}, as shown in Fig. 7. For the unbalanced case, a stop-band occurs between $\omega_{\Gamma 1}$ and ω ω_{M2}. The stop-band disappears for the balanced case and $\omega_{\Gamma 1} = \omega_{\Gamma 2} = \omega_0$.

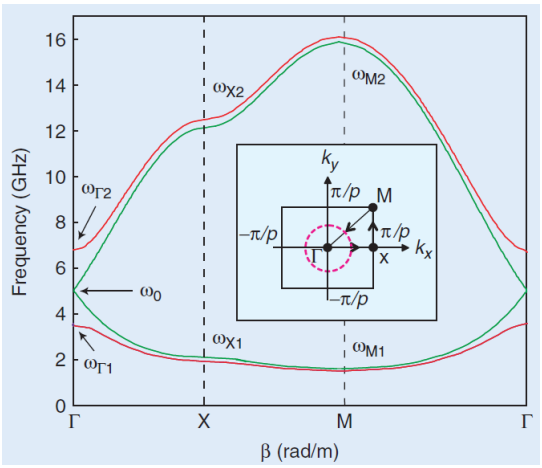

Fig. 7 Dispersion diagram for a balanced (green) and unbalanced (red) 2-D CRLH TL.

3. Applications

3.1. Phase Shifting

In positive refractive index media, since the group velocity and also phase velocity are in the same direction, the forward waves result in positive phase shift (phase lag) in the direction of positive group velocity. On the other hand the negative phase shift in the direction of positive group velocity is produced in the left handed media where the phase velocity and group velocity are in opposite directions (the backward waves). Therefore, one can imagine that the combination of the positive and negative refractive index media which is the basis of the NRI TL can realize arbitrary positive, negative or zero phase shift over a very short physical length compared to the wavelength of the operation frequency. However, the dispersion diagram shows the band gap originating from equation of the effective permittivity and permeability because the region that permittivity and permeability have opposite signs are not allowed. To avoid the bandgap, the two cutoff frequencies (which obtains from the frequency where the permittivity and permeability is zero) are equal. This dictates following relation where the Z0 is the positive refractive index TL. C_0 and L_0 are load capacitor and inductor for realizing the NRI TL, respectively.

$$\beta_{eff} \approx \omega\sqrt{LC} + \frac{-1}{\omega\sqrt{L_0 C_0}d}$$

This idea was implemented in [26] using lumped elements. The fabricated structure and the measured results are shown in Fig. 8. As it can be seen the 10 degree phase shifter realized using the NRI TL performs significantly better than normal transmission line and is relatively similar to the ideal 10^0 phase shifter

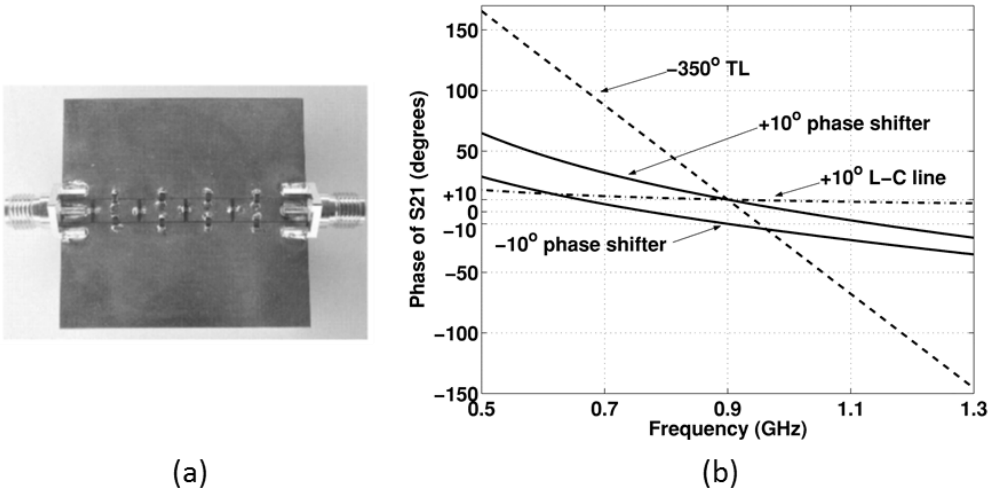

Fig. 8 a) Fabricated structure b) Comparison of the phase shift between NRI TL and normal transmission lines [26]

3.2. Antenna Design

The capability of realizing different phases over a wide range of frequency on a short length opens up a wide range of application. One of the major applications is to realize high performance antenna structure in terms of beam quality and bandwidth. Two major antenna categories in which NIR TL has been employed are 1) series fed antenna arrays and 2) leaky wave antennas.

In series fed antenna array, the NRI TL are utilized for the feeding network. In fact, zero phase shift lines are connected to the antenna elements to excite them in phase and generate the maximum beam perpendicular to the antenna surface. On can intentionally use constant phase difference for series fed array to have a main beam in a particular direction. Interestingly, due to the wide bandwidth of NRI TL the variation in main beam direction is mitigated significantly (reduction in beam-squinting). Therefore the antenna array pattern depends on the frequency mostly through the dependency of the antenna elements to the frequency and feeding network dependence on frequency is significantly reduced. Therefore, wideband antenna array can be realized by using wide band array elements such as bow tie antenna. In addition, this method leads to the more compact antenna structure due to the fact that instead of having the zero phase lines with one wavelength length, very short length of NRI-TL is used. Furthermore, an inter-element spacing of less than a half a free-space wavelength is necessary to avoid grating lobes in the visible region of the array pattern. NRI-TL alleviates this constraint as well.

One example of this type of antenna is implemented in [27]. An array of printed dipole antenna on microstrip technology is excited by using NRI-TL which is much smaller compared to its counterpart with normal zero phase transmission line. The measurement results also show very low beam squinting compared to the normal transmission line as shown in Fig. 9.

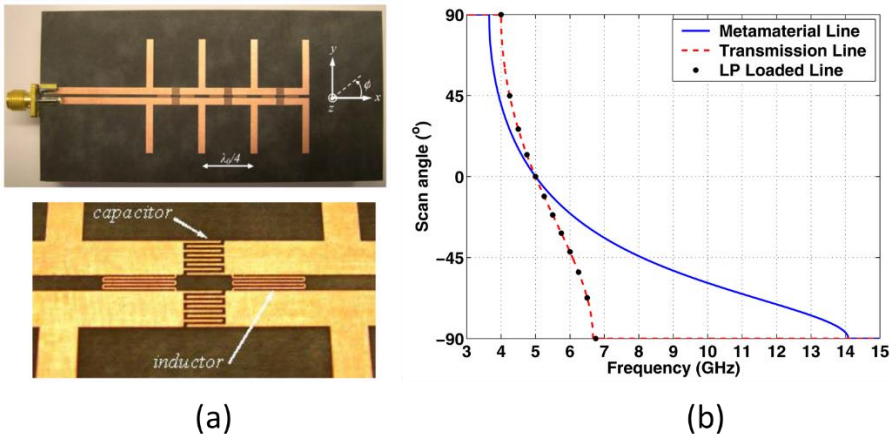

Fig. 9 a) The fabricated structure b) measurement results to compare NRI TL and normal TL in terms of beam squinting [27]

The other application of NRI TL is in the leaky wave antennas. These structures can be modeled as an infinitely long periodic structure that radiates to the free space through n=-1 space harmonic. However, one of the main difficulties of periodic LWAs is the significant deterioration of their radiation performance at broadside due to the presence of an open stopband where the leakage

constant drops to zero. NRI metamaterial unit cells are of much interest to build quasi-uniform LWAs, which radiate the n=0 harmonic at the backward region, broadside, and forward region.

One example of reduced beam-squinting leaky wave antenna is demonstrated in [28]. The proposed structure consists of cascade of NRI TLs with meandered inductor and interdigitated capacitor. The structure is implemented on coplanar strip line technology. The fabricated structure and measurement results are shown in Fig. 10. The paper confirms that a LWA with reduced beam squinting can be achieved when each of the constituent NRI-TL unit cell operates in the upper RH region, where the phase response of the NRI-TL line is the most linear, and group velocity is closest to the phase velocity.

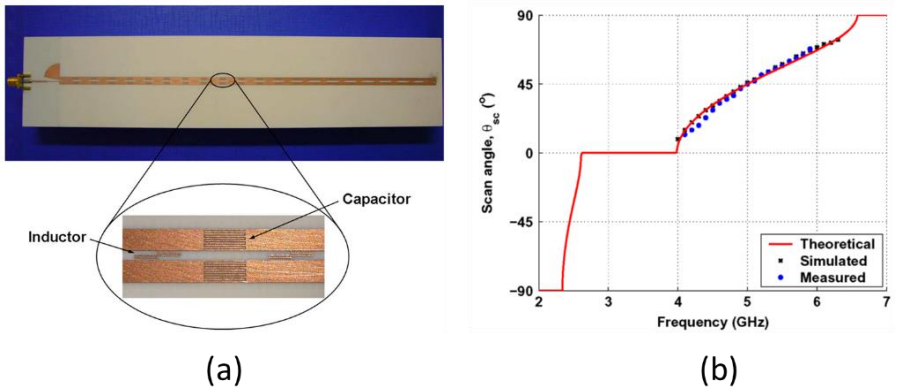

Fig. 10 a) The fabricated structure b) measurement results for beam angle which shows low beam squinting [28]

Another recent example of NRI TL based leaky wave antennas is shown in [29]. The structure that is implemented on co planar waveguide utilizes new cells called "supercells" instead of traditional NRI unit cell. The supercells have lower inductance which leads to less complex structure and lower resistive loss. Consequently, antenna shows improved efficiency and gain although it operates over narrower bandwidth compared to the traditional ones.

3.3. Perfect Imaging

Improving the image resolutions of the lenses is one of the application of NRI structures. In fact normal lenses show limited resolution which is fundamental to their performance and is called diffraction limit. Diffraction limits states that the minimum feature size in the image is larger than the wavelength of the monochromatic wave. In fact, this limit is expressed as follows:

$$\Delta R = \frac{2\pi}{k_{t\_max}} \xrightarrow{For\ positive\ refractive\ index} \Delta R = \frac{2\pi}{k} = \lambda$$

Where ΔR is the spatial resolution and k_{t_max} is the maximum transvers wave number for propagating waves. This limitation coming from the fact that the normal lenses only works for the propagating waves with real propagation constant which results in real incident angles to the lens surface. On the other hand, normal lenses attenuate the evanescent waves with imaginary

propagation constant substantially. However, the part of the wave which is needed to reconstruct the small features is evanescent and would not be captured by normal lenses.

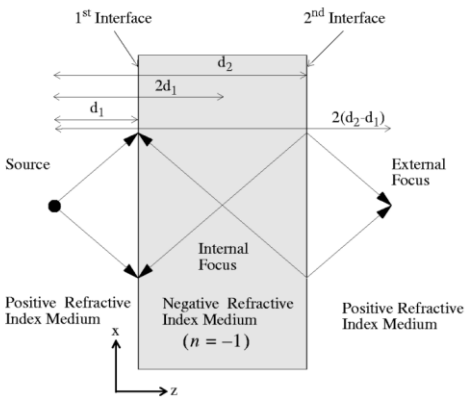

Fig. 11 The flat lens based on NRI medium [30]

Employing NRI based structure can resolve this problem. As first time it was shown by Velasgo, the slab NRI material acts as a peculiar lens where it focuses the waves emanating from a point source as shown in Fig. 11. Later, Pendry demonstrated that the NRI slab enhances the evanescent field which can be a solution to achieve perfect imaging. In fact if the NRI medium is lossless, impedance matched and has refractive index of -1 respect to the surrounding media perfect imaging can be achieved. The conditions reflects the fact that the enough evanescent wave should reach to the NRI region. Therefore, as well as aforementioned conditions, the source itself should be close enough to the NRI region, otherwise the attenuating field would be very week at the interface and would be lost in the noise floor of the system. The typical distance is in the range of $\lambda/2$.

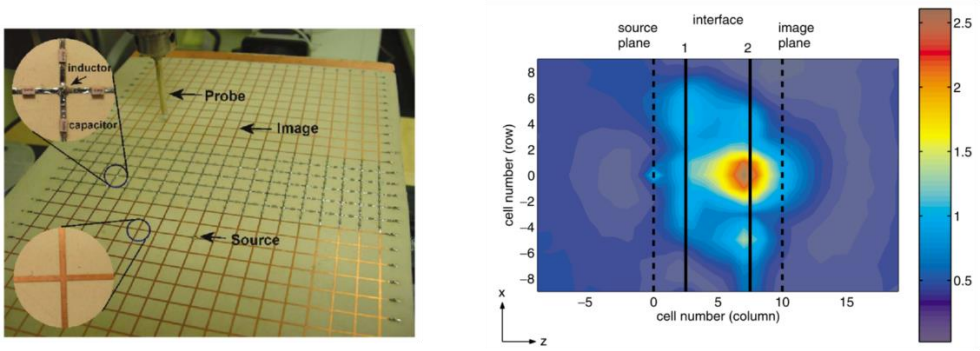

Fig. 12 a) fabricated structure ond planar NRI based lens b) Measure vertical electric field [31]

The planar type of such structure can be implemented using the NRI TL which benefits from low loss. Fig. 12a shows one practical implementation of this planar lens comprising a region with 2D NRI TL network and two other unloaded transmission line network on its both side with normal dispersion curve. The conditions for perfect imaging can be obtained to satisfy Pendry's conditions. The two networks can have impedance matched by equating the block wave impedance

of the unloaded and NRI structures. In addition, opposite permittivity of the regions is achieved by making refractive index the intrinsic wavenumber k, in the unloaded network and the one in the 2-D NRI TL equal in magnitude but opposite in sign.

Analysis of this structure shows that k_{t_max} can be larger from the wave number of the media by the factor of $ln(Q_c)/kh$ where Q_c is the quality factor of the loading series capacitor and h is the thickness of the NRI TL network (NIR lens). This relation reveals that the higher Q and electrically thinner (smaller kh) lenses lead to higher resolution.

As expected and also confirmed by the measurement results in Fig. 12b, the analysis of this lens demonstrates the enhancement of the evanescent fields in the lens. However, interestingly, this enhancement happens up to a certain thickness and after that the structure will not support the wave number larger than k.

In a more recent publication [32], this idea is extended and is used to achieve subwavelength focusing. A planar 2-D loaded microstrip TL which realizes hyperbolic metamaterial with very flat dispersion is employed. The subwavelength focusing up to $\lambda_g/19$ at 1GHz is achieved.

3.4. Couplers

One example of the NRI based coupler is shown in Fig. 13 which consists of one microstip line and one NRI TL [33]. Based on the coupled mode theory, the wave couples from one line to the other at the frequency that the propagation constant of the two line are equal. The dispersion curve of the NRI based coupler shows stop band region where the propagation constant of the two lines are the same. Therefore, there would exist complex mode in transmission lines with exponential decay of the power. In fact the microstrip line continuously leaks power backward to the NRI TL. This exponential decay leads to higher coupling efficiency over a relatively short distance. Creation of the stop band happens when a mode in a periodic structure couples to a higher order backward waves. But in this case, the fundamental spatial harmonics of two lines are involved.

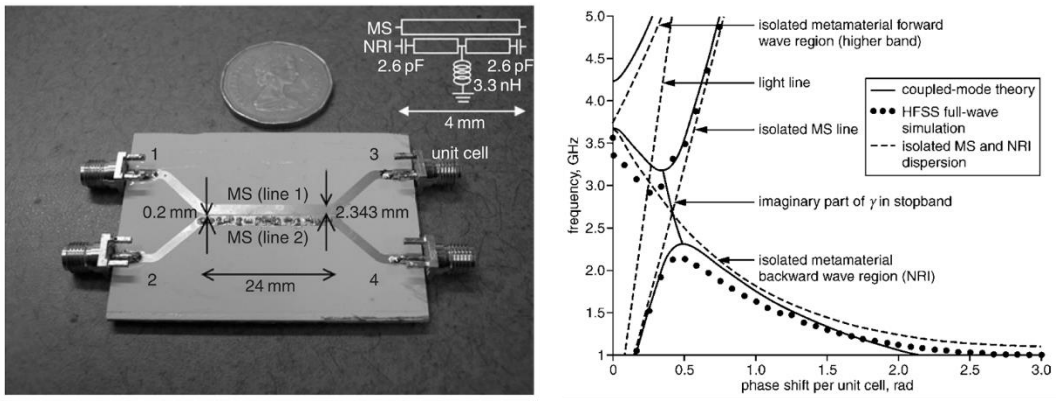

Fig. 13 a) fabricated structure of the coupler b) Dispersion diagram of the coupler obtained using coupled mode theory and also HFSS simulations [33]

The complex conjugate propagation constants ($\alpha \pm j\beta$) in the stop band region demonstrate complex conjugate impedances ($Z_0 \pm j\Delta Z$). One can write the following expression for s-parameters of this 4 port coupler when the excitation is at port 1. Port2, port3, and port4 are the coupled, through and isolated, respectively.

$$S_{11} = j\frac{\Delta Z}{Z_0} tanh(\alpha D) \qquad S_{21} = j\, tanh(\alpha D)$$

$$S_{31} = e^{-j\beta D}\, sech(\alpha D) \qquad S_{41} = j\frac{\Delta Z}{Z_0} sin(\beta D)\, sech(\alpha D)$$

Where D is the coupler length. Due to the exponential nature of the tangent hyperbolic function, most of the power can be coupled to the other line for a length of few $1/\alpha$. Also it can be noticed from the S_{41} expression that perfect isolation can be achieved for a length which is an integer multiple of half wavelength (corresponding to the propagation constant of the line). The comparison of the measurement results for NRI based and conventional coupler reveals better coupling efficiency and matching for the NRI based one.

3.5. Power Dividers

The other application of the NRI TL can be seen in the power dividers. Basically, power dividers can be implemented in two different topologies, corporate feed and series feed. The series feed has the advantage of more compact realization as the binary-tree corporate-fed networks can be collapsed into a single feed line. They also exhibits higher efficiency and lower losses (conductor and dielectric) due to the smaller foot print. However, using the traditional TL limits the operating bandwidth considerably due to the frequency dependence of the TL.

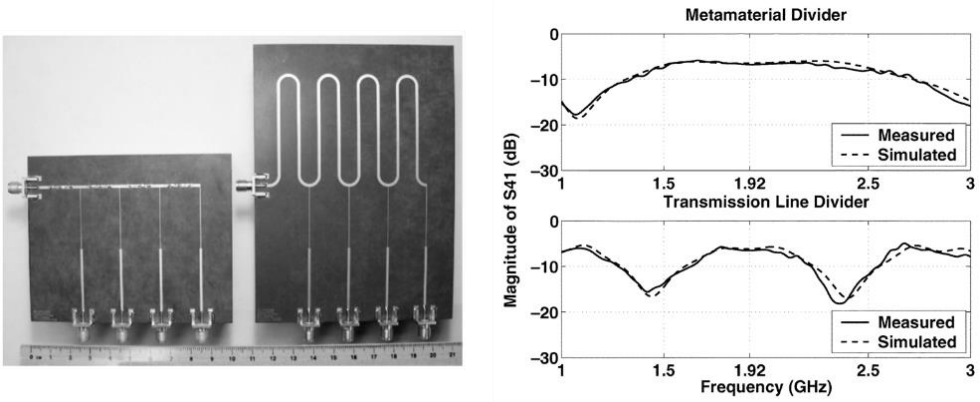

Fig. 14 a) The fabricated structure b) measurement results for one of the output ports to compare the bandwidth of NRI TL power divider with normal TL power divider [34]

By applying the NRI TL, the bandwidth can be improved significantly as shown in [34]. This kind of structure can be used in power amplifier to increase the output power and also for antenna arrays. Fig. 14a shows the fabricated structures using NRI TL and normal TL. The size reduction

is noticeable. The comparison measurement result is depicted in Fig. 14b which confirms the bandwidth extension in the case of NRI TL.

A modification to the structure is presented in [35] to increase the isolation between the output port which is essential for increasing the number output ports.

The flatness of the phase difference can be even improved further by having an asymmetrical power divider as proposed in [36]. As shown in Fig. 15, the paper uses asymmetrical T-structure power divider to compensate the nonlinear phase difference between the metamaterial and conventional transmission line.

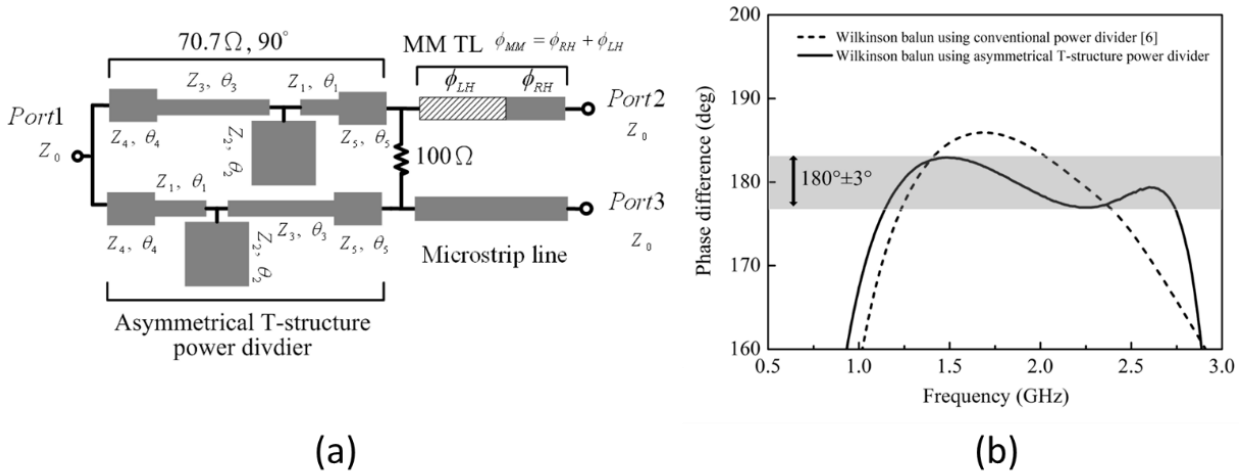

Fig. 15 a) Proposed asymmetric power divider in b) Comparison of the measurement result with traditional NI TL based power divider [36]

3.6. Balun

Wideband baluns also can be realized using the NRI TL. Baluns are need for the antenna in general devices with differential inputs. One popular example in microwave range is two wire antenna. One topology is proposed in [37] using microstrip line and is shown in Fig. 16. In this design, the input power is split using a Wilkinson power divider. One output should see 90 degree phase shift and the other -90 degree. The phase shifts are realized by metamaterial phase shift lines with broadband characteristics. The positive 90 degree phase shift is realized on the negative refractive index region (backward wave) while the negative phase shift operate on positive refractive index region (forward wave). In order to have the differential signal at the output of the balun over a wide bandwidth, the phase shift lines are designed to have the same slop. Lastly, the propagation constant of the both forward and backward waves are designed to results in slow waves which do not radiate into free space. The simulation results are shown in Fig16.b for output differential phase which shows superior performance for NRI TL based balun.

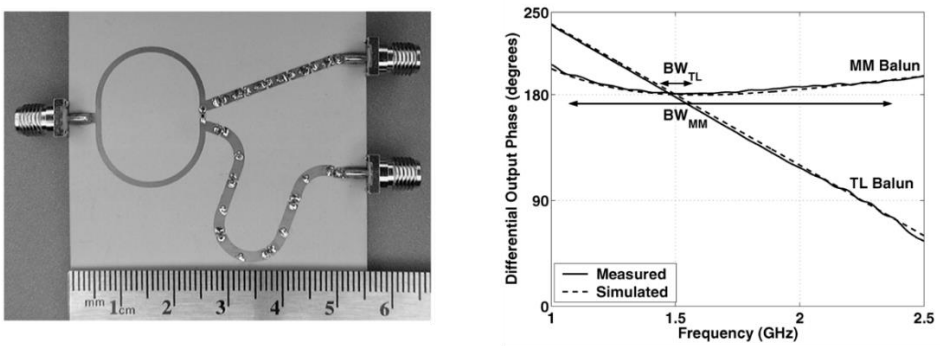

(a) (b)

Fig. 16 a) fabricated structure b) simulation results for output differential phase which shows superior performance for NRI TL based balun

4. Advantages and Disadvantages

This section discusses first the advantage and then disadvantages of NRI TL. Besides the general advantages of the metamaterials structure which leads to a wide range of new applications, the NRI-TL based metamaterials benefits mainly from wide left-handed (backward-wave) pass bands and comparably low insertion losses. The advantages originates from the absence of resonant elements used to synthesize the negative permeability. This is opposed to the first metamaterial structures where the resonant elements were utilized as the key components. To clarify the absence of the resonant structure which explains the broadening of the bandwidth in NRI-TL media stems from the fact that their constituent C-L resonators are tightly coupled together through their electrical connections. Also NRI TL can be easily implemented on the low cost planar transmission lines which makes the fabrication in large quantity feasible.

NRI transmission lines offer great versatility in terms of their phase response that can be tailored to any specification, and their size which can be made arbitrarily small. Therefore they can be used in any structure with transmission line to reduce the overall size and improve the performance due to the unique properties of the metamaterials. In fact, applying NRI TL to the circuits is very straight forward as most of the microwave circuits are based on or have part of transmission line. So, NRI TL based structures can be easily integrated to the existing designs and they eliminate the need for coupling the light from one type of media to another.

Regarding the disadvantage of NRI TL, as the technology and the devices move toward higher frequencies more serious challenges encounter the design of the NRI TL. Especially, because in the most of the implementations, the transmission lines are loaded with the lumped components which might quite lumped at higher frequencies. Also, the period d is very small compared to the wavelength which results in more challenges for fabrication of NRI TL at higher frequencies.

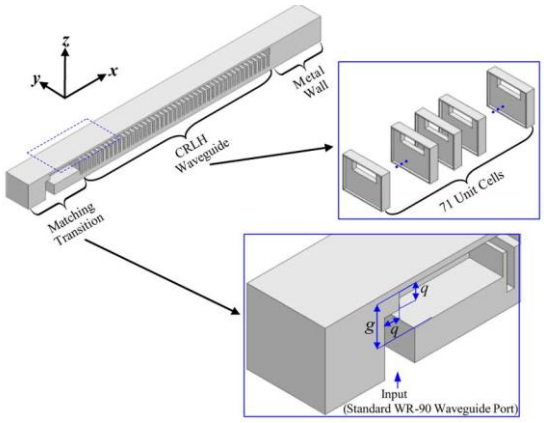

Fig. 17 The proposed NRI TL based rectangular waveguide for high power applications [38]

Additionally, most present CRLH transmission lines are based on planar circuit, such as microstrip, stripline and coplanar waveguide, which have already been used to realize many novel microwave components. Being cheap and easy to fabricate are the main benefits of using these

kind of CRLH transmission lines. However, they inherently can handle limited amount of power and their application are limited to low power one.

However, the rectangular waveguides can be used address higher power applications. One such structure as Slotted-Waveguide Antenna is designed and tested in [38]. However, a sophisticated 3D structure, as shown in Fig. 17, is needed to implement the loaded capacitance an inductance in the transmission line. This type of structure would be very complex and lead to a very expensive and complicated fabrication process. Specially, moving toward higher frequency results in very fine feature that cannot be easily manufactured. The advent of the 3D printer might be a solution for this obstacle which is more pronounced for high power applications.

5. Future Directions

In general, NRI TL field has reached to a point of maturity where the proof of concept of many novel components such as antenna, coupler, lenses and concepts such as high resolution imaging has demonstrated. Therefore, the researcher should put one step further and embark on the real problem in the industry.

One such area that stands to benefit tremendously from the use of metamaterial technology is compact and hand-held electrical devices. There are stringent requirements for the size of the different components such as the antennas and phase shifters especially the ones for the next-generation broadband wireless communication systems. For instance, the requirements for the antennas in the new standards are in general high efficiency and compact size that can conform to the size requirements of handheld wireless devices, as well as multi-band operation within the existing wireless standards.

Additionally, as well as passive structures, the active NRI TL structure can be an important topic for the future research. The feasibility of improving the bandwidth and realizing electronically tunable systems using the active components can be studied and applied to the components that have so far implemented using metamaterial structures. One example is the NRI TL based antennas where the active phase shifter can be employed to realize beam forming for radar and communication applications.

Another possible future research can be in investigation of the bulk (3D) metamaterial structure. Currently, the design and fabrication of these kind of structures imposes major challenges that should be overcome.

Finally, there still tremendous theoretical work can be done in this area. Especially many designs have conducted using only superficial circuit and EM simulation using the commercial software. For example, Several aspects of the MS/NRI-TL coupled-line system that need further studies include the effects of loss, dispersion and the modelling of electrically large loading elements.

6. Conclusion

This report presented an overview on the particular type of metamaterial structure called negative refractive index transmission line where the metamaterial structure with all amazing properties is realized using the loaded transmission line with series capacitance and parallel inductors. The underlying theory was described for both 2D and 3D structures.

Additionally, different application of NRI TL was also demonstrated to prove the superior performance of the NRI TL based structure. One of the main building blocks based on the metamaterial which is zero phase shift line was explained in details. Other application such as power divider, balun, and Antenna arrays which are mainly based on zero or negative phase shift line were presented. Especially for the antenna structure it was shown that higher gain with smaller structure can be realize using NRI TL. Finally, it was shown that subwavelength imaging is possible using a NRI lenses by retrieving evanescent fields which carry subwavelength image information. The NRI lens is comprised of a NRI region sandwiched between two positive refractive index regions. The section elaborated on the unique property of the NRI lens that can enhance the evanescent fields emanating from the object and focus the beams on the other side of the lens.

The advantages and disadvantages of the metamaterials particularly NRI TL were also discussed. NRI TL are low loss and wide band due to absence of the resonance structures to synthesize the negative permeability. However, there still challenges for implementing them for high power application as well as high frequency one. Finally, few possible future research areas were introduced.

References

1. “Breakthrough of the year: The runners-up,” Science, vol. 302, no. 5653, pp. 2039-2045, 2003.

2. N. Engheta and R. W. Ziolkowski (editors), *Metamaterials: Physics and Engineering Explorations*, N. Engheta, R. W. Ziolkowski, Editors, IEEE Press, Wiley Inter-Science, New York, 2006.

3. *IEEE Transactions on Antennas and Propagation*, Special Issue on Metamaterials, vol. 51, no. 10, October 2003.

4. G. V. Eleftheriades and K. G. Balmain (editors), *Negative-Refraction Metamaterials: Fundamental Principles and Applications*, John Wiley & Sons, New York, 2005.

5. G.V. Eleftheriades and M. A. Antoniades, “Antenna Application of Negative Refractive Index Transmission Line (NRI-TL) Metamaterials,” Chapter 14, in *Modern Antenna Handbook*, C. A. Balanis (editor), John Wiley & Sons, pp. 677–736, 2008.

6. R. Marques, F. Martin, and M. Sorolla, *Metamaterials with Negative Parameters: Theory, Design and Microwave Applications*, John Wiley & Sons, New York, 2008.

7. C. Caloz and T. Itoh, *Electromagnetic Metamaterials: Transmission Line Theory and Microwave Applications*, John Wiley & Sons, New York, 2006.

8. R. Porath, "Theory of miniaturized shorting-post microstrip antennas," IEEE Transactions on Antennas and Propagation, vol. 48, no. 1, January 2000, pp. 41-47.

9. J. H. Lu and K. L. Wong, "Slot-loaded meandered rectangular micros trip antenna with compact dual frequency operation," Electronic Letters, vol. 34, May 1998, pp. 1048-1050.

10. D. H. Schaubert, D. M. Pozar, and A Adrian, "Effect of microstrip antenna substrate thickness and permittivity," IEEE Transactions on Antennas and Propagation, vol. 37, no. 6, June 1989, pp. 677-682.

11. J. C. Bose, “On the rotation of plane of polarization of electric wave by a twisted structure,” Proc. Roy. Soc., vol. 63, pp. 146–152, 1898.

12. I. V. Lindell, A. H. Sihvola and J. Kurkijarvi, “Karl F. Lindman: The last Hertzian and a Harbinger of electromagnetic chirality,” IEEE Antennas Propagat. Magazine, vol. 34, no. 3, pp. 24–30, 1992.

13. W. E Kock, “Metallic delay lines,” Bell Sys. Tech. J., Vol. 27, pp. 58–82, 1948.

14. V. G. Veselago, “The electrodynamics of substances with simultaneous negative values of ε and μ,” Sov. Phys.-Usp., vol. 47, pp. 509–514, Jan.–Feb. 1968.

15. J. B. Pendry, A. J. Holden, W. J. Stewart and I. Youngs, “Extremely, low-frequency plasmons in metallic mesostructure,” Phys. Rev. Letters., vol. 76, pp. 4773–4776, June 1996.

16. J. B. Pendry, A. J. Holden, D. J. Robbins, and W. J. Stewart, “Low-frequency plasmons in thin wire structures,” J. Phys., Condens. Matter, vol. 10, pp. 4785–4809, 1998.

17. J. B. Pendry, A. J. Holden, D. J. Robbins, and W. J. Stewart, “Magnetism from conductors and enhanced nonlinear phenomena,” IEEE Trans. Microwave Theory Tech., vol. 47, no. 11, pp. 2075–2081, Nov. 1999.

18. J. B. Pendry, “Negative refraction makes a perfect lens,” Phys. Rev. Lett ., vol. 85, pp. 3966–3969, Oct. 2000.

19. D. R. Smith, W. J. Padilla, D. C. Vier, S.C. Nemat-Nasser, and S. Schultz, “Composite medium with simultaneously negative permeability and permittivity,” Phys. Rev. Lett., vol. 84, pp. 4184–4187, May 2000.

20. D. R. Smith, D. C. Vier, N. Kroll, and S. Schultz, “Direct calculation of the permeability and permittivity for left-handed metamaterials,” Appl. Phys. Lett., vol. 77, pp. 2246–2248, Oct. 2000.

21. D. R. Smith and N. Kroll, “Negative refractive index in left-handed materials,” Phys. Rev. Lett., vol. 85, pp. 2933–2936, Oct. 2000.

22. R. A. Shelby, D. R. Smith, S. C. Nemat-Nasser, and S. Schultz, “Microwave transmission through a two-dimensional, isotropic, left-handed metamaterial,” Appl. Phys. Lett., 78, pp. 489–491, Jan. 2001.

23. A. Shelby, D. R. Smith, and S. Schultz, “Experimental verification of a negative index-of-refraction,” Science, vol. 292, pp. 77–79, April 2001.

24. G.V. Eleftheriades, “Analysis of bandwidth and loss in negative-refractive-index transmission-line (NRI-TL) media using coupled resonators,” IEEE Microw. Wireless Compon. Lett., vol. 17, no. 6, pp. 412–414, Jun. 2007.

25. C. Caloz and T. Itoh, "Composite right/left-handed transmission line metamaterials", IEEE Microwave Magazine. pp. 34-50, 2004.

26. M. A. Antoniades and G. V. Eleftheriades, "Compact linear lead/lag metamaterial phase shifters for broadband applications," in *IEEE Antennas and Wireless Propagation Letters*, vol. 2, no. 1, pp. 103-106, 2003.

27. M. A. Antoniades and G. V. Eleftheriades, "A Metamaterial Series-Fed Linear Dipole Array with Reduced Beam Squinting," *Antennas and Propagation Society International Symposium 2006, IEEE*, Albuquerque, NM, 2006, pp. 4125-4128.

28. M. A. Antoniades and G. V. Eleftheriades, "A CPS Leaky-Wave Antenna With Reduced Beam Squinting Using NRI-TL Metamaterials," in *IEEE Transactions on Antennas and Propagation*, vol. 56, no. 3, pp. 708-721, March 2008.

29. A. Mehdipour and G. V. Eleftheriades, "Leaky-Wave Antennas Using Negative-Refractive-Index Transmission-Line Metamaterial Supercells," in *IEEE Transactions on Antennas and Propagation*, vol. 62, no. 8, pp. 3929-3942, Aug. 2014.

30. A. Grbic and G. V. Eleftheriades, "Negative refraction, growing evanescent waves, and sub-diffraction imaging in loaded transmission-line metamaterials," in *IEEE Transactions on Microwave Theory and Techniques*, vol. 51, no. 12, pp. 2297-2305, Dec. 2003.

31. A. Grbic and G. V. Eleftheriades, "Overcoming the diffraction limit with a planar left-handed transmission-line lens," Phys Rev Lett. Mar. 2004.

32. S. H. Sedighy, C. Guclu, S. Campione, M. K. Amirhosseini and F. Capolino, "Wideband Planar Transmission Line Hyperbolic Metamaterial for Subwavelength Focusing and Resolution," in *IEEE Transactions on Microwave Theory and Techniques*, vol. 61, no. 12, pp. 4110-4117, Dec. 2013.

33. R. Islam, F. Elek and G. V. Eleftheriades, "Coupled-line metamaterial coupler having co-directional phase but contra-directional power flow," in *Electronics Letters*, vol. 40, no. 5, pp. 315-317, 4 March 2004.

34. M. A. Antoniades and G. V. Eleftheriades, "A broadband series power divider using zero-degree metamaterial phase-shifting lines," in *IEEE Microwave and Wireless Components Letters*, vol. 15, no. 11, pp. 808-810, Nov. 2005.

35. R. Islam and G. V. Eleftheriades, "Compact Corporate Power DividerUsing Metamaterial NRI-TLCoupled-Line Couplers," in *IEEE Microwave and Wireless Components Letters*, vol. 18, no. 7, pp. 440-442, July 2008.

36. C. Lin and C. H. Tseng, "Metamaterial-based Wilkinson balun using asymmetrical T-structure power divider for improving phase response flatness," *Microwave Conference Proceedings (APMC), 2012 Asia-Pacific*, Kaohsiung, 2012, pp. 19-21.

37. M. A. Antoniades and G. V. Eleftheriades, "A broadband Wilkinson balun using microstrip metamaterial lines," in *IEEE Antennas and Wireless Propagation Letters*, vol. 4, no. , pp. 209-212, 2005.

38. S. Liao *et al*., "Synthesis, Simulation and Experiment of Unequally Spaced Resonant Slotted-Waveguide Antenna Arrays Based on the Infinite Wavelength Propagation Property of Composite Right/Left-Handed Waveguide," in *IEEE Transactions on Antennas and Propagation*, vol. 60, no. 7, pp. 3182-3194, July 2012.